

Supporting Information

Free-Standing Two-dimensional Sheets of Polymer-Linked Nanoparticles

*Xiaole Hu, Ji-eun Park, Seulki Kang, Chan-Jin Kim, Youngji Kim, Jerome Kartham Hyun,
and So-Jung Park**

Department of Chemistry and Nanoscience, Ewha Womans University, 52 Ewhayeodae-gil,
Seodaemun-gu, Seoul, 03760, Korea.

* Correspondence to: sojungpark@ewha.ac.kr

Materials. The monomer (tert-butyl acrylate) and RAFT agent (4-cyano-4-[(dodecylsulfanylthiocarbonyl)sulfanyl] pentanoic acid (RAFT-2.0)) were purchased from the Sigma-Aldrich. The initiator (4,4'-azobis(4-cyanovaleric acid) (V-501)) was purchased from Alfa Aesar and used as received. Poly(vinyl alcohol) (PVA_{9,000-10,000}, 80 % hydrolyzed), poly(ethylene oxide) (PEO, 60,000 g/mol), poly(acrylamide) (PAAm, 150,000 g/mol), poly(sodium 4-styrenesulfonate) (PSS₃₄₃, ~70,000 g/mol) and PEDOT:PSS (1.0 wt. % in water) were purchased from Sigma-Aldrich and used without any further treatment.

Iron chloride hexahydrate (FeCl₃·6H₂O, 98%), sodium oleate (≥99%), oleyamine (OAm, technical grade), gold chloride trihydrate (HAuCl₄·3H₂O), sodium borohydride (NaBH₄, ≥98%), tetraoctylammonium bromide (TOAB, 98%), 1-dodecanethiol (DT, ≥98%), cadmium oxide (CdO, 99.99%), selenium powder (99.5%, powder), sulfur (99%, powder), 1-octadecene (ODE, 90% technical grade), stearic acid (95%), octadecylamine (OLAm, 90%), tri-n-octylphosphine (TOP, 97%), trioctylphosphine oxide (TOPO, 99%), 1-octanethiol (>98.5%), octadecylamine (ODA, 90% technical grade) and oleic acid (OA, 90% technical grade) were purchased from Sigma-Aldrich. Octadecylphosphonic acid (ODPA, 99%) and hexylphosphonic acid (HPA, 99%) were purchased from Polycarbon Industries. Borane tert-butylamine complex (95%, Acros), 1,2,3,4-tetrahydronaphthalene (97.0 %, TCI). Organic solvents were purchased from the Sigma-Aldrich or Daejung Chemicals and used as received.

Instrumentation. Molecular weights (Mn) and polydispersity index (PDI) of synthesized polymers were estimated by gel permeation chromatography (GPC) system (Shimadzu) setting at 40 °C with a flow rate of 1 mL/min, using THF as eluent and polystyrene standards. Chemical structures of synthesized polymers were determined by proton nuclear magnetic resonance (¹H NMR) on a Bruker Avance 300 MHz NMR spectrometer. Fourier transform infrared spectroscopy (FT-IR) was measured with Varian 800. Fluorescence spectra were measured with the Perkin Elmer 5S 55 fluorescence spectrometer. Extinction spectra were obtained by

using UV-visible spectrophotometer equipped with a temperature controller system (Agilent Technologies). Transmission electron microscopy (TEM) images were taken using JEM-2100F electron microscope (JEOL Ltd.) operating at 200 kV accelerating voltage. Optical microscope image was taken using Olympus BX51 instrument. Atomic force microscope (AFM) image was taken from Park system (XE7) instrument with non-contact mode. Raman measurements were carried out on a micro-Raman spectrometer (LabRam HREvo 800, HORIBA Jobin Yvon) using 633 nm laser.

Finite-difference time-domain (FDTD) simulations. FDTD simulations were performed to calculate the electric field distribution of a single AuNP and AuNP array. A plane wave at 633 nm, polarized along the x-direction was normally injected onto the plane of the array. Periodic and PML boundary conditions were used for the lateral (x,y) and normal (z) dimensions, respectively. Optical constants for Au and Si (the substrate) were obtained from Johnson and Christy and Palik, respectively.

Synthesis and characterization of nanoparticles and polymers. Iron oxide nanoparticles (IONPs) with varying diameters (5.2 ± 0.4 nm, 9.5 ± 0.8 nm, 14 ± 0.7 nm) were synthesized by the thermal decomposition method.¹ CdSe (3.2 ± 0.5 nm) quantum dots (QDs) were synthesized by the hot injection method.² CdSe/CdS core/shell QDs (15 ± 1 nm) were synthesized by the subsequent shell growth by the successive ionic layer adsorption and reaction (SILAR).³ CdSe/CdS core/shell quantum rods (QRs) (length: 5.2 ± 0.7 nm, width: 58 ± 9 nm) were synthesized by the well-established seeded-growth method.⁴ Oleyamine-stabilized gold nanoparticles (AuNPs, 5.2 ± 0.4 nm) was synthesized by the modified Brust method, respectively.⁵ The size of nanoparticles was determined by TEM. Characterization data of synthesized nanoparticles are presented in Figure S1-4.

Poly(acrylic acid) (PAA) was prepared by the hydrolysis of poly(*tert*-butyl acrylate) (PtBA) synthesized by the reversible addition-fragmentation chain-transfer (RAFT)

polymerization, following a previously reported method.⁶ The characterization data of synthesized polymers are presented in Figure S5-6. Molecular weights of PtBA₆₉ (9,200 g/mol, PDI=1.11) and PtBA₂₄₃ (31,500 g/mol, PDI=1.09) were measured by GPC.

Synthesis of oleic acid-capping iron oxide nanoparticle. Iron oxide nanoparticles were synthesized by the widely used thermal decomposition method.¹ The iron-oleate precursor was prepared by refluxing 5.4 g iron chloride hexahydrate (FeCl₃·6H₂O) and 18.25 g sodium oleate in a solvent mixture composed of 30 mL water, 40 mL ethanol and 70 mL hexane in 250 ml round flask for four hours. The iron-oleate was washed with 250 mL water three times by centrifugation at 5,000 rpm for 5 min. 2.05 g iron oleate and 0.5 g oleic acid were mixed in 20 mL 1-octadecane in a 100 ml two-neck round flask. The solution was heated to 80 °C, degassed for 30 min under N₂, heated to 320 °C at a constant heating rate of 3.3 °C /min, and kept at the temperature for 30 min. Then size of nanoparticles was controlled by varying the ratio between the iron precursor and oleic acid ligand. The synthesized nanoparticles were washed with acetone 4-5 times after cooling down to room temperature and characterized by TEM (Figure S1).

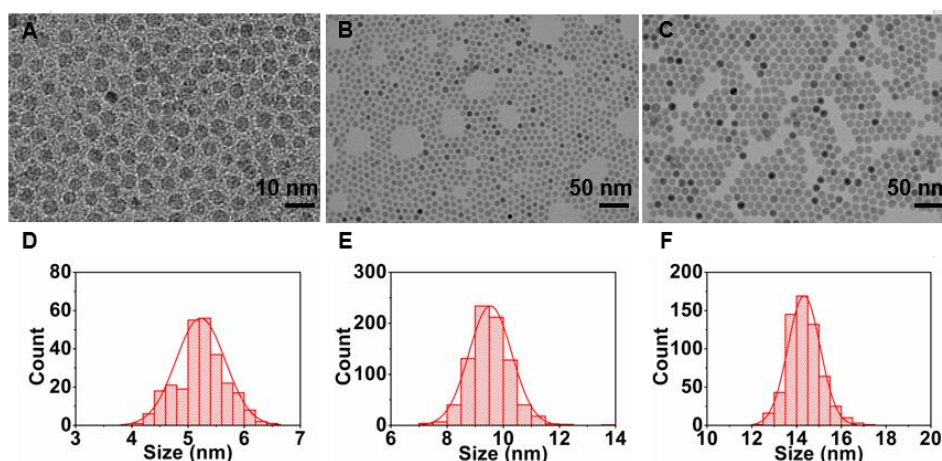


Figure S1. TEM images (A-C) and size histogram (D-F) of iron oxide nanoparticles with diameters of 5.2 ± 0.4 nm (A, D), 9.5 ± 0.8 nm (B, E) and 14 ± 0.7 nm (C, F).

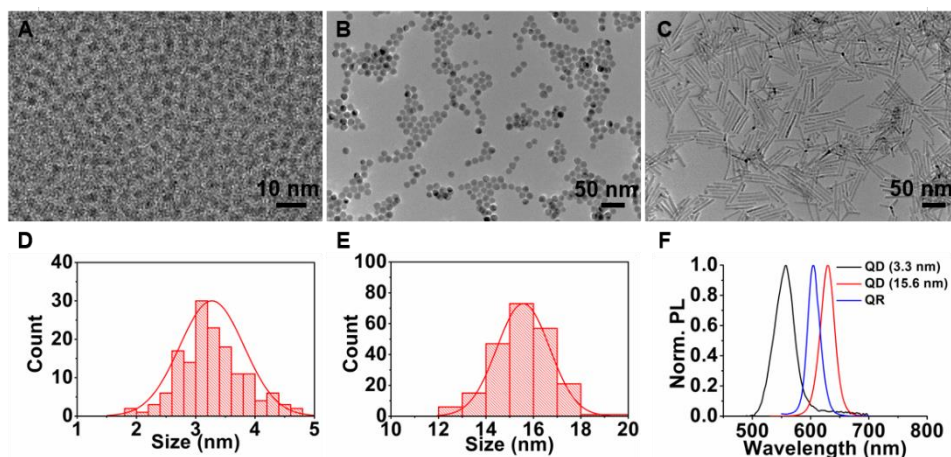


Figure S2. (A-B) TEM images of QDs with diameters of 3.2 ± 0.5 nm (A) and 15 ± 1 nm (B). (C) TEM image of QRs with the length of 5.2 ± 0.7 nm and width of 58 ± 9 nm. (D-E) Size histograms of 3.2 nm (D) and 15 nm (E) QDs shown in (A) and (B), respectively. (F) normalized photoluminescence spectra of QDs and QRs (3.2 nm CdSe QDs ($\lambda_{\text{ex}}=488$ nm, $\lambda_{\text{em}}=556$ nm), 15 nm CdSe/CdS QDs ($\lambda_{\text{ex}}=516$ nm, $\lambda_{\text{em}}=629$ nm), QRs ($\lambda_{\text{ex}}=516$ nm, $\lambda_{\text{em}}=604$ nm)).

Synthesis of 5.2 nm AuNP. AuNPs stabilized with oleylamine were synthesized by a previously reported method.⁵ In a typical method, a solution containing borane-tert-butyl amine complex (48 mg), oleylamine (1 mL), and 1,2,3,4-tetrahydronaphthalene (1 mL) was injected into the precursor solution of gold chloride hydrate (0.1 g), oleylamine (10 mL), and 1,2,3,4-tetrahydronaphthalene (10 mL) under stirring. The mixture was allowed to react at room temperature for 1 h. The synthesized nanoparticles were washed by the centrifugation (8,000 rpm, 10 min) after the precipitation with acetone and 1:3 hexane/acetone mixture. Then, the precipitates were redispersed in chloroform. Extinction coefficient (ϵ) of 1.16×10^7 L·mol⁻¹·cm⁻¹ was used for the calculation of nanoparticle concentration.⁷

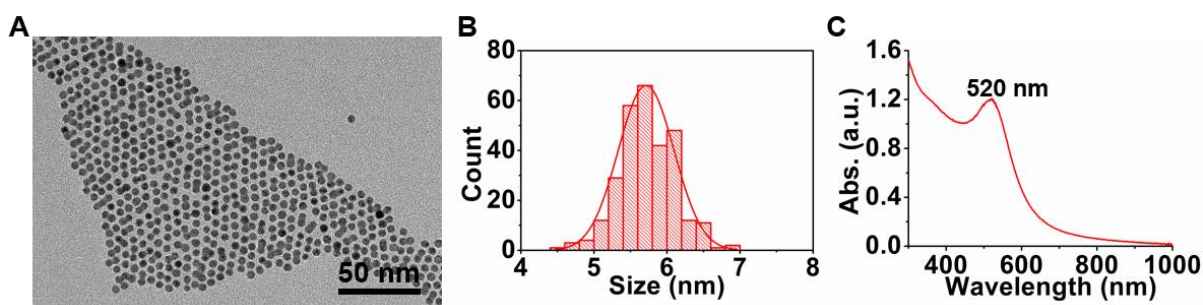


Figure S3. TEM image (A), size histogram (B), and extinction spectra (C) of AuNPs with the diameter of 5.2 ± 0.4 nm.

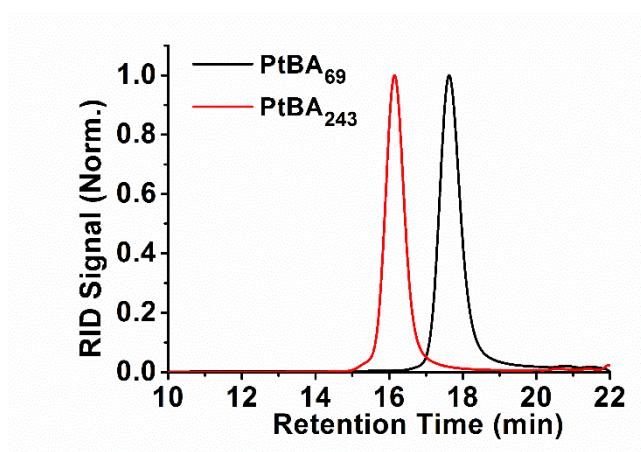


Figure S4. GPC chromatogram of PtBA.

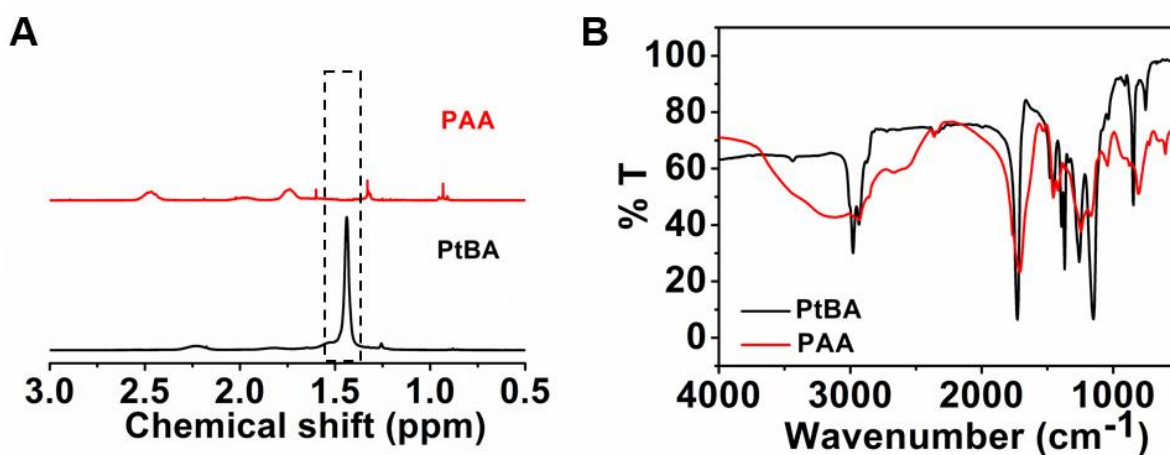


Figure S5. (A) ^1H NMR spectra of PtBA and PAA. (B) FT-IR spectra of PtBA (black line) and PAA (red line).

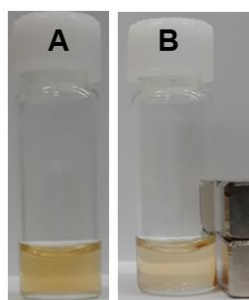


Figure S6. Magnetic attraction test of 5.2 nm IONP/PAA₆₉ nanosheets in water (B). A photograph of a nanosheet solution without a magnet is presented in (A) for comparison.

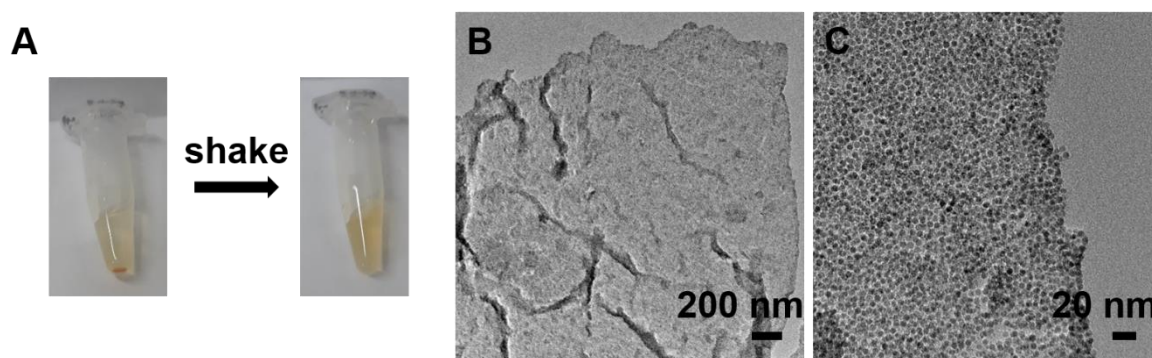


Figure S7. Stability of 5.2 nm IONP/PAA₆₉ nanosheets in water ~one year after the preparation. (A) Photographs showing that precipitated 2D nanosheets can be redispersed in water by gentle shaking. (B-C) TEM images of 2D nanosheets showing the intact assembly structure.

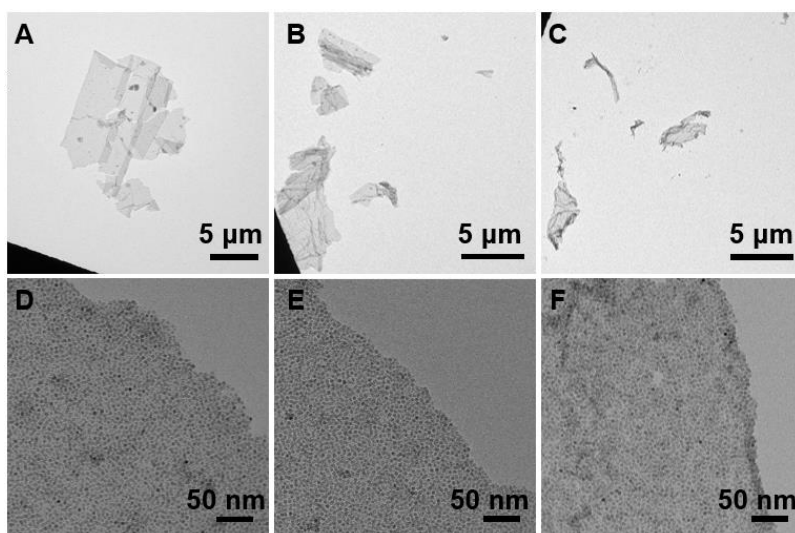


Figure S8. The effect of relative nanoparticle/polymer concentration on 2D assembly. TEM images of 2D sheets formed at varying nanoparticle concentrations of 0.02 mg/mL (A, D), 0.1 mg/mL (B, E), and 0.4 mg/mL (C, F) at a fixed PAA concentration of 1.5 mg/mL. 5.2 nm IONP/PAA₆₉ pair was used for the experiments. Well-defined nanosheets were formed for the nanoparticle concentration range from 0.02 to 0.2 mg/mL with high transfer efficiencies to water. When the nanoparticle concentration was higher than about 0.2 mg/mL, significant amounts of particles remained in the chloroform phase (Figure S10), although nanosheets were still found in the water layer.

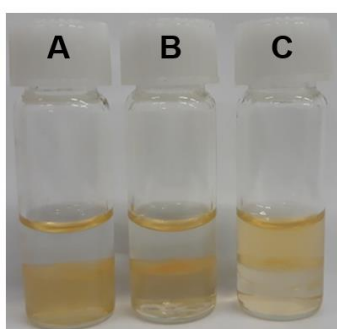


Figure S9. The effect of polymer concentration on 2D assembly. The experiments performed at varying polymer concentrations ((A) without PAA, (B) 0.01 mg/mL, (C) 0.1 mg/mL) show that the transfer efficiency depends on the polymer concentration. 5.2 nm IONP/PAA₆₉ pair was used for the experiments. The IONP concentration was set to 0.2 mg/mL.

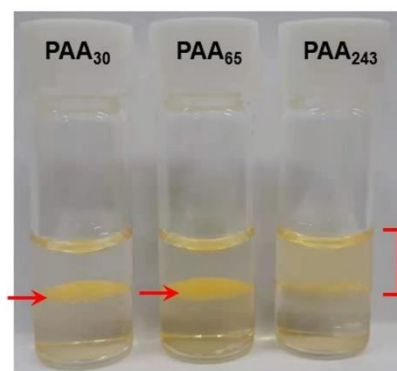


Figure S10. PAA length effect on the 2D assembly and transfer of 15 nm QDs. The opaque yellow coloration of the top water phase shown in the PAA₂₄₃ sample is indicative of the transfer of nanoparticle assemblies into the water phase. PAA₃₀ and PAA₆₅ induced accumulation of QDs at the interface. However, QDs remain at the interface without significant amounts of QDs in the water phase, as evidenced by the lack of yellow color in the water phase.

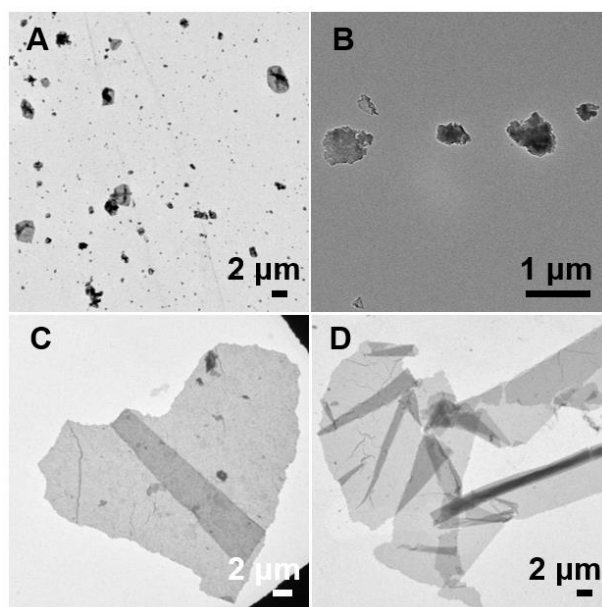


Figure S11. pH effect on the self-assembly of IONP/PAA₆₉: (A) potassium chloride/hydrochloric acid buffer (pH 1.8), (B) potassium chloride/hydrochloric acid buffer (pH 3.4), (C) phosphate/citrate buffer (pH 5), and (D) sodium borate buffer (pH 9). 5.2 nm IONPs were used for A, C, and D. 6 nm IONPs were used for B.

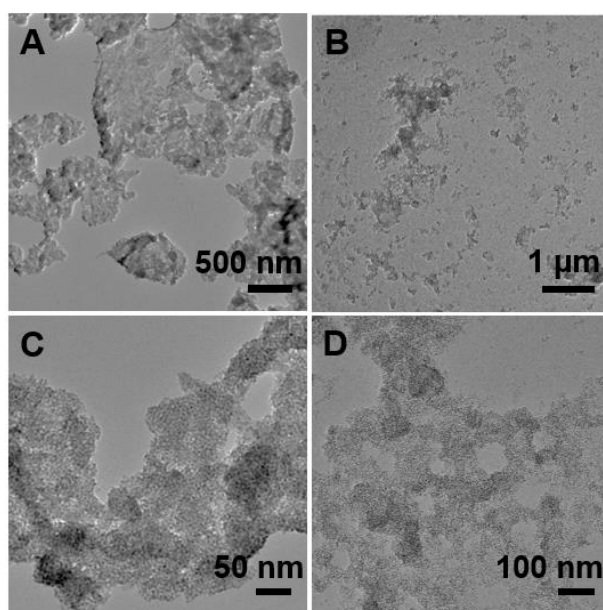


Figure S12. TEM images of IONP/PEO (A, C), IONP/PVA (B, D) assemblies.

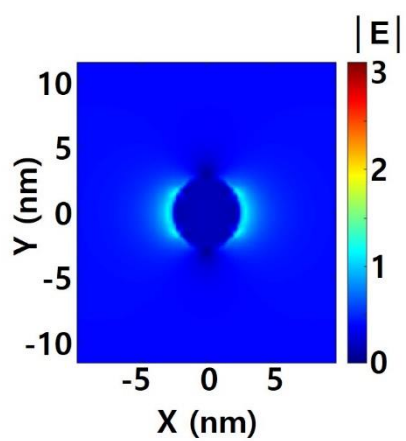


Figure S13. Near-field electric field distribution on an isolated AuNP on a silicon substrate under the illumination of 633 nm, x-polarized incident light.

References

1. J. Park, K. An, Y. Hwang, J. G. Park, H. J. Noh, J. Y. Kim, J. H. Park, N. M. Hwang and T. Hyeon, *Nat. Mater.*, 2004, **3**, 891-895.
2. O. Chen, J. Zhao, V. P. Chauhan, J. Cui, C. Wong, D. K. Harris, H. Wei, H. S. Han, D. Fukumura, R. K. Jain and M. G. Bawendi, *Nat. Mater.*, 2013, **12**, 445-451.
3. J. J. Hao, J. Zhou and C. Y. Zhang, *Chem. Commun.*, 2013, **49**, 6346-6348.
4. L. Carbone, C. Nobile, M. De Giorgi, F. D. Sala, G. Morello, P. Pompa, M. Hytch, E. Snoeck, A. Fiore, I. R. Franchini, M. Nadasan, A. F. Silvestre, L. Chiodo, S. Kudera, R. Cingolani, R. Krahne and L. Manna, *Nano Lett.*, 2007, **7**, 2942-2950.
5. S. Peng, Y. Lee, C. Wang, H. Yin, S. Dai and S. Sun, *Nano Res.*, 2008, **1**, 229-234.
6. X. Hu, C. J. Kim, S. K. Albert and S. J. Park, *Langmuir*, 2018, **34**, 14342-14346.
7. J. Shang and X. Gao, *Chem. Soc. Rev.*, 2014, **43**, 7267-7278.